CARBON 50 (2012) 1753–1761

Available at www.sciencedirect.com

SciVerse ScienceDirect

journal homepage: www.elsevier.com/locate/carbon

Improved graphitization and electrical conductivity of suspended carbon nanofibers derived from carbon nanotube/polyacrylonitrile composites by directed electrospinning

Tanmoy Maitra [a], *Swati Sharma* [b], *Alok Srivastava* [a], *Yoon-Kyoung Cho* [b], *Marc Madou* [b,c], *Ashutosh Sharma* [a,d,*]

[a] *Department of Chemical Engineering, Indian Institute of Technology, Kanpur 208016, U.P., India*
[b] *School of Nano-Bioscience and Chemical Engineering, UNIST, Ulsan 689-798, South Korea*
[c] *Department of Mechanical & Aerospace Engineering, University of California, Irvine, CA 92697-3975, United States*
[d] *School of Mechanical Engineering, Yeungnam University, Gyongsan 712749, South Korea*

ARTICLE INFO

Article history:
Received 26 July 2011
Accepted 8 December 2011
Available online 16 December 2011

ABSTRACT

Single suspended carbon nanofibers on carbon micro-structures were fabricated by directed electrospinning and subsequent pyrolysis at 900 °C of carbon nanotube/polyacrylonitrile (CNT/PAN) composite material. The electrical conductivity of the nanofibers was measured at different weight fractions of CNTs. It was found that the conductivity increased almost two orders of magnitude upon adding 0.5 wt.% CNTs. The correlation between the extent of graphitization and electrical properties of the composite nanofiber was examined by various structural characterization techniques, and the presence of graphitic regions in pyrolyzed CNT/PAN nanofibers was observed that were not present in pure PAN-derived carbon. The influence of fabrication technique on the ordering of carbon sheets in electrospun nanofibers was examined and a templating effect by CNTs that leads to enhanced graphitization is suggested.

1. Introduction

Graphitic carboneous materials often have a distribution of crystalline domains [1] that allow free movement of electrons for increased conductivity [2,3]. The use of macro, micro and nano graphitic carbons in a variety of applications, including next generation electronics [4–9], activated carbon fibers [10], composite materials [9,11], batteries [12–14], fuel cells [15,16], sensors [17,18] etc., are being extensively studied. The methods to obtain more graphitic carbon structures in nanoscale devices by using less complicated and less expensive fabrication techniques is thus an attractive area of exploration.

Chemically or physically imposed graphitization in bulk carbon materials, as well as in miniaturized structures, has been investigated for more than five decades [19,20]. Chemical methods of catalysis mostly include mixing metal additives [19,20] in the starting material, which can be a carbonizable polymer precursor, or an already pyrolyzed non-graphitic or semi-graphitic carbon. Although these inorganic additives lead to a fairly high proportion of graphitic domains in the resulting carbons, large amounts of remaining undesired metal component often limit the applications and industrial usage of these materials. Physical catalysis or templating, such as by filling a polymer precursor in confined areas like pores of a host structure [21] or by depositing them over Si surfaces [22–24], has also been explored as an effective way of obtaining more crystalline carbon. However, there is much less freedom of designing a device in this case as the template

* *Corresponding author at:* Department of Chemical Engineering, Indian Institute of Technology, Kanpur 208016, U.P., India.
E-mail address: ashutos@iitk.ac.in (A. Sharma).
0008-6223/$ - see front matter
doi:10.1016/j.carbon.2011.12.021

itself has a pre-defined geometry. To overcome these problems, it is desirable to use a carboneous templating material as an additive in the polymer precursor that yields highly graphitic carbon needing no further purification, and retains its flexibility for the design and fabrication of a device. To this end, we show CNT to be an efficient template for graphitization in PAN (polyacrylonitrile)-derived carbon. The resulting CNT–PAN composite is also suitable for a variety of micro- and nano-fabrication techniques.

Mechanical, electrical and electrochemical properties of CNT-polymer bulk composites and films as a result of increased ordering of carbon atoms have been investigated for a range of applications [6,25–32]. The properties of CNT-polymer composites are found to be dependent on a number of factors such as CNT-polymer interaction, extent of dispersion, orientation, size, shape, volume fraction and distribution of the CNTs in the polymer matrix [31,33–40].

In this study, we use controlled electrospinning for the fabrication of single, suspended CNT–PAN composite nanofibers that are seamlessly integrated with an underlying polymeric micro-electro-mechanical system (MEMS) platform. Pyrolysis of such structures produces carbon nanowires of tunable graphitic content and electrical conductivity anchored on and integrated with the underlying carbon micro-structure. Electrospinning is the most effective and the most widely used technique for the fabrication of thin mats of polymer nanofibers [26,28]. In the past several decades, different types of organic polymers and inks have been successfully processed as nanofibers using this technique, with typical examples including various engineering plastics, biopolymers, electrically conductive polymers, and fluorescent polymers [41,42]. PAN is a common polymer used for the production of CNF (carbon nanofiber) by pyrolysis because of the following advantages: (1) high carbon yield, (2) easy carbonization process, (3) surface of carbonized PAN nanofiber can be modified or functionalized, and (4) nanofiber papers can be utilized directly as electrode materials [11,28,42].

It is known that thin films and nanofiber mats obtained by mixing carbon nano-tubes in PAN solutions display increased conductivity with an increase in the concentration of CNTs. Guo et al. investigated the effect of concentration and nature of CNT (multi-walled carbon nanotube (MWCNT) or single-walled carbon nanotube (SWCNT)) on electrical conductivity of CNT/PAN composite films [28]. In similar work by Chen et al., CNTs were modified by plasma treatment and then acrylonitrile was grafted on the surface of CNTs [11]. Ra et al. investigated the effect of pyrolysis conditions and CNT loading on the electrical conductivity of CNT/PAN derived anisotropic nanofiber mats and discovered that the conductivity values were higher along the spinning direction [6]. They also reported that the increase in conductivity occurs not only because of the addition of CNTs (0.5–10 wt.%), but it also results from an increase in the carbonization temperature from 800 °C to 1000 °C. In all of the previous characterizations of the composite fibers, the four-probe method was used for the measurement of electrical conductivity, because the fibers were available only in the forms of fiber mats or films.

In the next generation of applications of CNF, e.g. in nanosensors, we envision positioning and integrating carbon nanowires with a variety of underlying MEMS/NEMS (nanoelectromechanical system) structures. The fabrication and properties of a single suspended composite carbon nanowire in such structures are yet to be established. Here, we report a greatly increased electrical conductivity and graphitization in electrospun carbon nanofibers (CNF) derived from homogeneously dispersed MWCNTs and PAN. We have recently reported a method for the self-assembled fabrication of a single suspended amorphous carbon nanowire on a carbon-MEMS platform by electrospinning and pyrolysis of PAN and SU 8 polymers [43]. Here, we explore this technique's potential to fabricate the CNT/PAN composite nanofibers anchored to electrodes and thus, investigate the graphitic and electrical properties of single suspended CNT/carbon composite nanofibers. The conductivity of electrospun carbonized CNT/PAN nanofibers is measured at four different concentrations of MWCNT in the PAN electrospinning solution. In order to understand the structural changes that are responsible for the increase in conductivity of these nanofibers, micro-Raman spectroscopy, X-ray diffraction (XRD) and high resolution transmission electron microscopy (HRTEM) are used. Our results indicate that the crystallinity and electrical conductivity of these composite nanofibers increase with increase in concentration of CNTs. An effective strategy for positioning, integration and interrogation of a single nanofiber requires controlled electrospinning as detailed elsewhere [43]. In this study, we also determine the maximum concentration of CNTs in PAN that allows good electrospinnability of the precursor polymer to carbon nanowires.

2. Materials and methods

Our overall fabrication methodology is a combination of three techniques: (1) photolithography to produce an SU 8 MEMS structure, (2) self-assembled electrospinning of functionalized CNTs in PAN solution to form nanowires anchored on the MEMS platform, and (3) controlled pyrolysis to obtain carbon composite wires integrated with the underlying carbon MEMS structure.

2.1. Chemicals

PAN (MW = 150,000) was obtained from Aldrich Chemical Company Inc. SU 8 2015 (Specific gravity 1.2, Micro Chem. Corporation, MA, USA) was used for the fabrication of the base C-MEMS structures upon which electrospun fibers were positioned. N, N-dimethyl formamide (DMF) (99% pure), utilized as the above polymer's solvent, was procured from Fischer Scientific.

2.2. Fabrication of SU 8 posts

An array of SU 8 posts (120 × 120 μm) was first fabricated by using standard photolithography [41,42,44] on a high resistivity p- type Si-wafer with a native SiO_2 layer. The height of

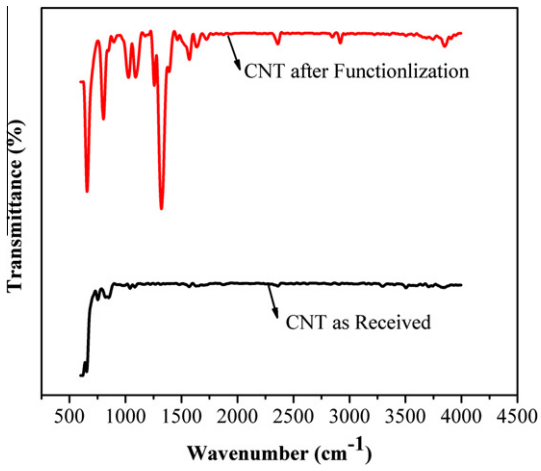

Fig. 1 – FTIR spectra of chemically treated and pristine MWCNTs.

these posts after pyrolysis was ~2 μm. Pyrolysis was carried out under the flow of N_2 at 900 °C.

2.3. *Synthesis and functionalization of CNTs*

MWCNTs were synthesized by catalytic chemical vapor deposition (CCVD). Fe/Co and magnesium carbonate were used as catalyst and support system, respectively. The temperature of the furnace was maintained at 900 °C and acetylene gas (97%) was used as the carbon source. The detailed conditions of the synthesis process are described elsewhere [45]. The average diameter of CNTs thus obtained was 25 nm with a length of up to 4 μm. CNTs were functionalized by refluxing with 3 M nitric acid solution at 110 °C and vigorous stirring for 4–5 h. Finally the nitric acid treated CNTs were dried in air at 120 °C to evaporate the residual solvent.

2.4. *Solution preparation and electrospinning*

Four different concentrations of CNTs in PAN for electrospinning were prepared by mixing 0.05, 0.1, 0.2 and 0.5 wt.% CNTs in 8 wt.% PAN in DMF. The detailed method for solution preparation is described elsewhere[6]. These solutions were electrospun using Dispovan® syringe (volume: 2.5 ml and diameter: 0.55 mm) at 13–15 kV on the SU 8 MEMS structures fabricated earlier. The distance between the tip of the jet and the SU 8 MEMS collector was 10 cm, and the flow rate of the solution was maintained at 1 μL/minute. Electrospinning was performed for a short period of 5–10 s to limit the number of wires and to obtain single wires suspended between posts. The resulting structures consisting of suspended composite nanowires on SU 8 posts were stabilized in air at 250 °C for 1 h prior to pyrolizing the whole structure which is done

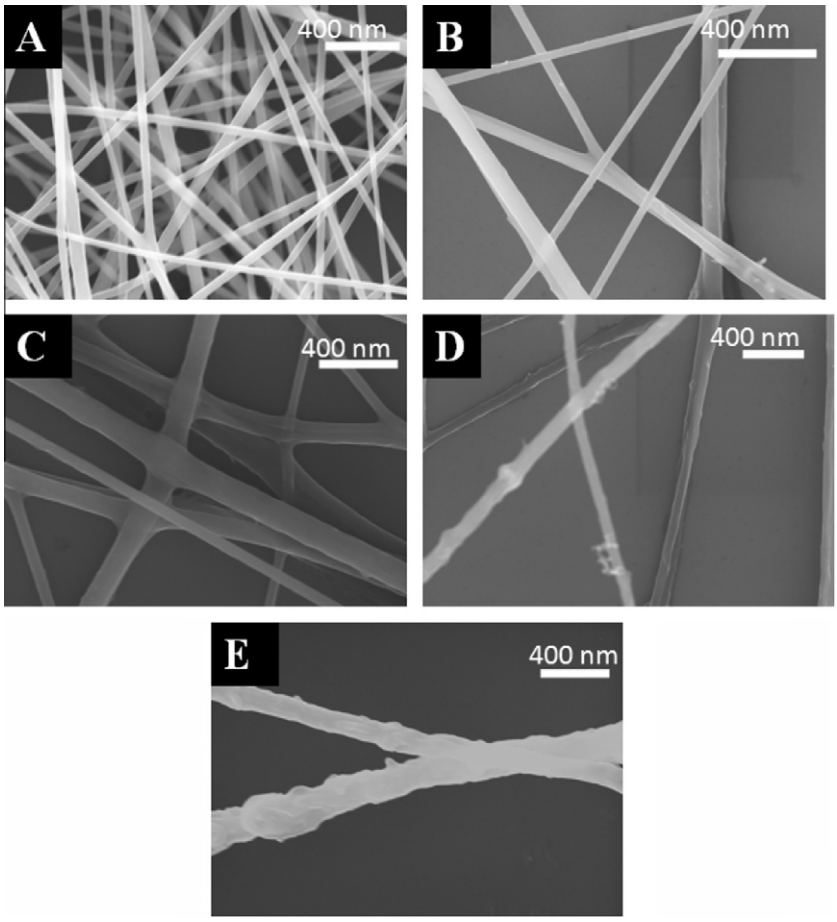

Fig. 2 – SEM micrographs of composite CNF derived from: (A) pure PAN, (B) 0.05% CNT in PAN, (C) 0.1% CNT in PAN, (D) 0.2% CNT in PAN, (E) 0.5% CNT in PAN.

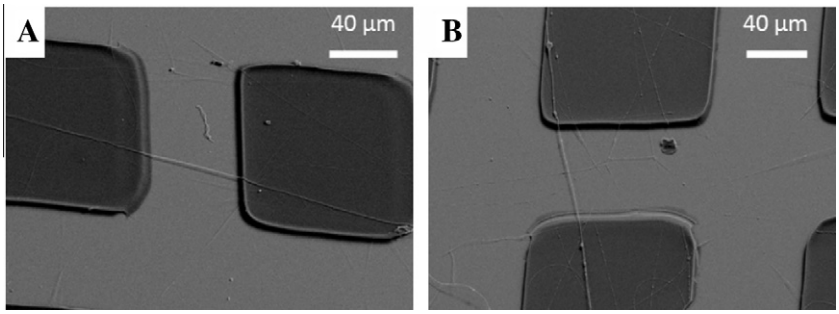

Fig. 3 – SEM micrographs of: (A) pure PAN, and (B) CNT/PAN composite derived CNFs suspended between carbon microposts (length, width and height of microsposts: ~225 μm, 200 μm and 2 μm, respectively. The gap between the posts is 75 μm).

under N_2 flow (flow rate: 0.2 L/min) at 900 °C for 1 h, with a ramp time of 5 °C/min, to yield a monolithic carbon structure having good interfacial contacts and with electrically conducting posts of much greater cross-sectional area than the nanofibers themselves.

2.5. *Conductivity measurements and structural characterizations*

The electrical conductivity of the thus fabricated suspended composite carbon nanowires between carbon posts was measured using a Keithley 6517A digital electrometer. Electrical contacts to the two carbon micro-posts were made with sharp tip micro-probes. Fourier transform infrared analysis for characterization of functional groups on CNTs was carried out on a TENSOR 27 Fourier transform infrared spectrometer (FTIR-ATR, Bruker Optik, GmbH, Germany) consisting of a DLaTGS detector with a germanium internal reflection element (IRE) crystal to compare pristine and nitric acid treated CNTs and verify their oxidation.

Field emission scanning electron microscopy (FESEM, Quanta 200, Zeiss, Germany) was utilized to characterize the surface morphologies of pure PAN and CNT/PAN derived carbon fibers. HRTEM (JEM-2100F JEOL, Japan) was carried out to confirm the presence of graphitic structures in the nanofibers fabricated as bulk mats on Si substrates. XRD studies (X'Pert PRO, PANanalytical, Netherlands) using Cu Kα radiation, were performed and Raman spectra (WiTec, Germany; $\lambda = 543$ nm) were obtained for pure and composite PAN-derived fibers in order to understand the change in the graphitic nature of the CNF as a function of the CNT weight fraction.

3. Results

Fig. 1 represents the FTIR spectra for pristine and nitric acid treated CNTs. The peaks identified at 1360, 1710 and 3402 cm^{-1} confirm the presence of C–O, C=O and O–H bonds in the CNT with surface modification [46].

Figs. 2 and 3 display the SEM micrographs of carbonized CNT/PAN mats and suspended nanofibers on carbon posts, respectively. It may be observed in Fig. 2-E that the fibers do not display a very smooth surface at concentrations higher than 0.5 wt.% CNTs in PAN. The average diameter for the nanofibers fabricated in bulk while using the same fabrication parameters was ~100 nm while the distribution of diameters ranged from 50 to 300 nm. Diameter of a single nanofiber spun on micro-posts was measured from electron micrographs along its length at several spots and averaged. When calculating the resistance and conductivity values of nanofibers, their individual diameters were used in the calculations as observed by FESEM. The conductivity values for pure PAN and CNT/PAN derived CNFs are reported in Fig. 4.

The nanofibers deposited on the SU 8 micro-structures displayed very good adhesion that may be visualized in the SEM micrographs. As indicated earlier, after deposition of single polymeric fibers on the array of SU 8 micro posts/pillars, the whole structure was subjected to stabilization in air at 250 °C for one hour prior to carbonization. The glass transition temperature of PAN and CNT/PAN composite fibers is in the range of 100–150 °C. Our own TGA measurements on the CNT/PAN composite fibers showed the glass transition to be complete below about 180 °C. Thus, stabilization also encourages fusion of fibers with the post. Further, pyrolysis produced a carbon monolithic structure which should further aid good integration. As a result, the I–V curves of the carbon composite fibers were ohmic. One can thus conclude that there is negligible contact resistance in the nanofibers fabricated by this route.

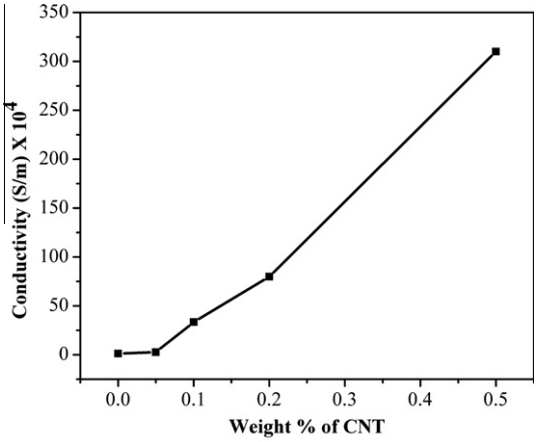

Fig. 4 – Conductivity of single suspended composite CNF. Conductivity of pure PAN, PAN +0.05% CNT, PAN +0.1% CNT, PAN +0.2% CNT and PAN +0.5%CNT nanowires are (in S/m $\times 10^{-4}$): 1.2 ± 0.0437, 2.65 ± 0.096, 33.3 ± 0.574, 80 ± 0.062 and 310 ± 2.7, respectively.

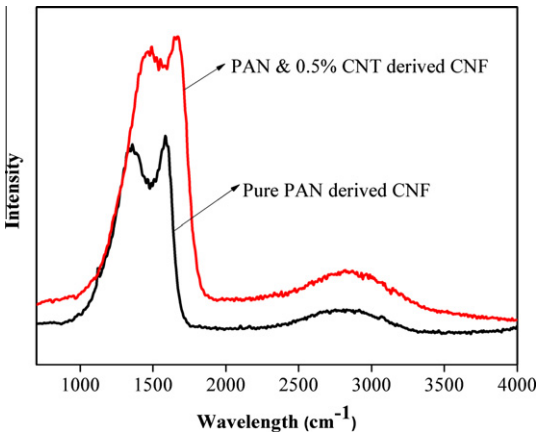

Fig. 5 – Raman spectra for the CNF derived from pure PAN and CNT/PAN (0.5 wt.% CNT) composite material.

Fig. 5 displays the representative Raman spectra for the CNF investigated in our experiments. It is well known that the ratio of G-band to D-band depends on both the degree of graphitization and the alignment of graphitic planes [6]. From the spectra, it was confirmed that the I_g/I_d value of composite nanofibers increased upon increasing the concentrations of CNTs. Interestingly, there is a spectacular rise of almost two orders of magnitude in the conductivity value at 0.5% CNT/carbon composite nanofibers compared to a pure PAN derived fiber. This may be ascribed to a greater nucleation of crystalline structures templated by the CNT in the composite fibers. A templated propagation during pyrolysis could help the fiber attain a more graphitic or crystalline structure. It is also observed in the HRTEM pictures displayed in Fig. 6 that the pure PAN derived nanofibers contain fewer discrete graphitic zones in the form of small crystals, but in the case of CNT/PAN composite, the crystalline domains increase in size. We could not, however, conclusively observe any differences in the crystal sizes at different concentrations of CNTs, as the region captured by HRTEM is very small (20–50 nm).

The crystallite size was also calculated by using the empirical formula, $L_a = C(\lambda)*(I_g/I_d)$, where L_a is the crystallite domain's size and C is a function of the laser wavelength ($C(\lambda) = 4.4$ nm) [11]. The results are listed in Table 1. As observed, the crystalline domain's size for CNT/PAN composite fiber increased from 0.970 ± 0.023 to 1.300 ± 0.009 on increasing the concentration of CNTs from 0 to 0.5 wt.% in PAN.

As it may be observed in Fig. 6-A, although PAN derived CNF also display some graphitization, the graphitic sheets in this case are not very well arranged and the crystallite's size is very small. In case of CNT/PAN composite (Fig. 6-B), the graphite crystals are well formed and the separation between planes is 0.34 nm as confirmed by the X-ray patterns integrated with HRTEM (Fig. 6-C).

To determine the length and continuity of these crystals and confirm the effect of templating caused by CNTs, we

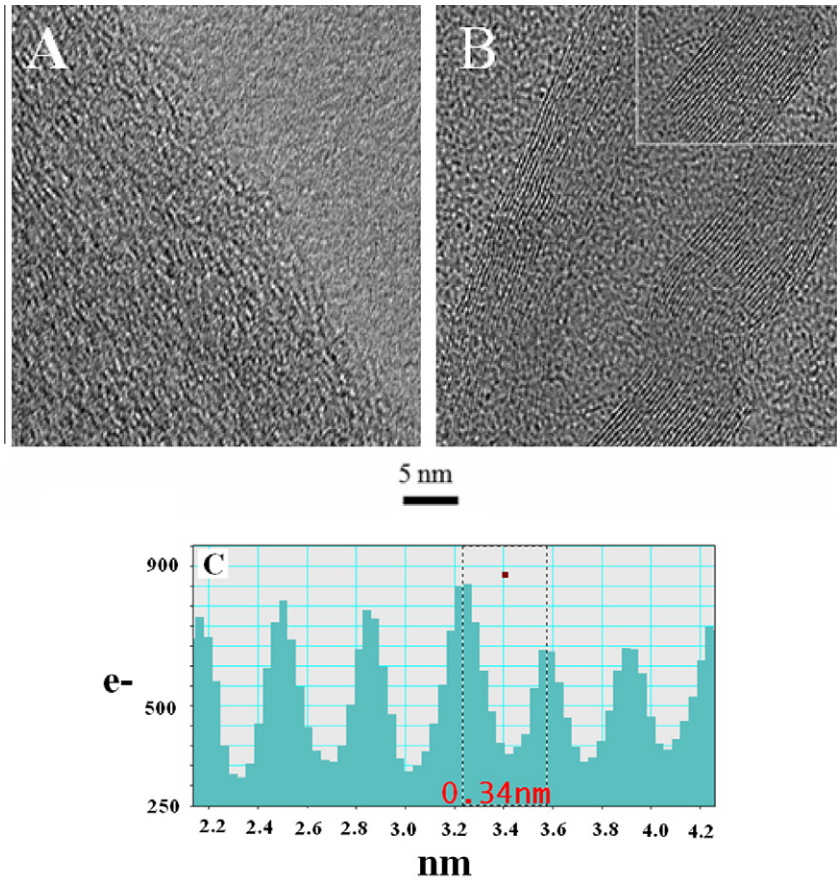

Fig. 6 – HRTEM images of: (A) pure PAN, and (B) CNT/PAN (0.5 wt.% CNT) derived CNF. (C) X-Ray diffraction patterns integrated with HRTEM showing the distance between graphitic planes in (B).

Table 1 – Graphitization and increase in crystallite size based on Raman spectra for CNF derived from pure PAN and CNT/PAN composite material.

Composition	I_g/I_d	$L_a = 4.4*I_g/I_d$ (nm)
Pure PAN-C	0.22 ± 0.0038	0.970 ± 0.023
PAN-C + 0.05%CNT	0.22 ± 0.0040	0.970 ± 0.024
PAN-C + 0.1%CNT	0.24 ± 0.0010	1.056 ± 0.006
PAN-C + 0.2%CNT	0.25 ± 0.0020	1.100 ± 0.012
PAN-C + 0.5%CNT	0.30 ± 0.0015	1.300 ± 0.009

carried out a detailed HRTEM analysis for CNT/PAN composite CNF. The results are displayed in Fig. 7(A–D). As is apparent from Fig. 7-A and B, the length of graphite crystals in the CNF is at least 100 nm, which is surprisingly higher than what we observed in pure PAN derived CNF (Fig. 6-A). Also, there is no signature of amorphous regions in this composite CNF material, which is characteristic of carbons with low graphite contents such as the pure PAN derived carbon. Fig. 7-C confirms the presence of CNTs in the resulting composite CNF and Fig. 7-D indicates the possibility of very high graphitization near the walls of CNTs.

We also carried out XRD analysis to determine the enhancement in graphitization in CNT/PAN derived CNF. The results are shown in Fig. 8. The broadening and increase in intensity of the peak at 2θ close to 27° for the 002 plane, and the graphitic peak for 004 plane at 2θ ~54° is much sharper which indicates better crystallinity in the case of the composite-CNF in comparison to the pure PAN derived CNF [19].

4. Discussion

The electrospun composite nanofibres self-assemble to connect the posts owing to a stronger electric field on their tips thus obviating the need for positioning and integration of carbon nanowires with the underlying microstructures and paving the way for fabricating novel carbon based micro and

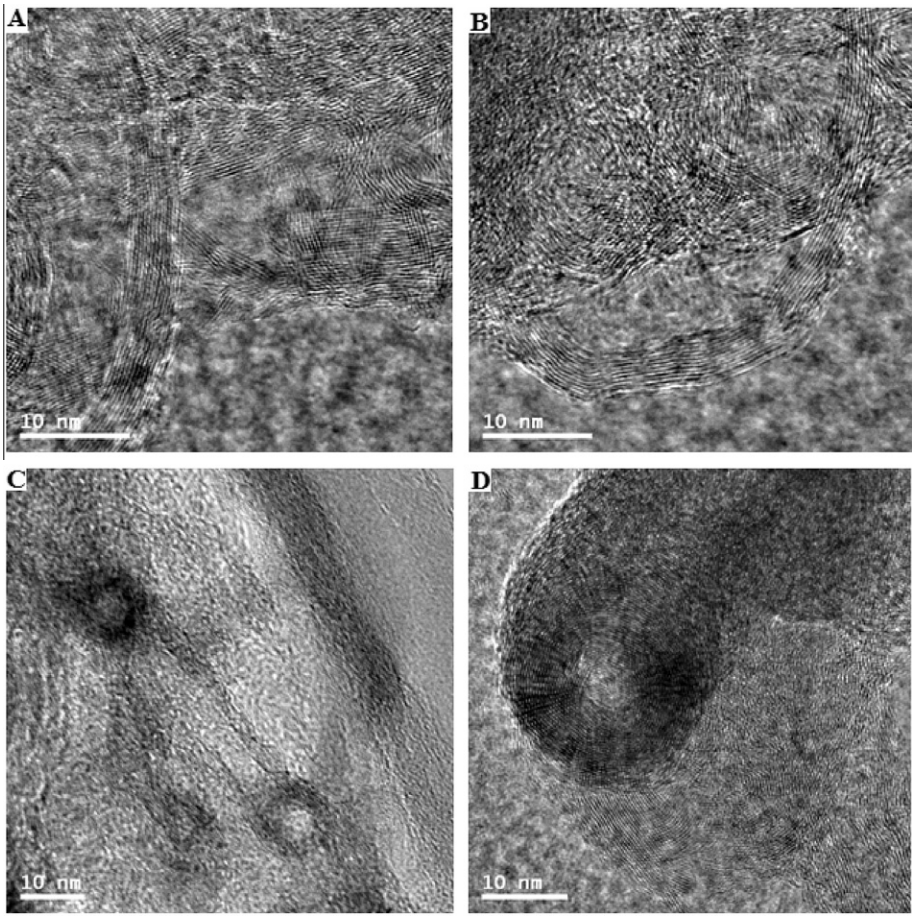

Fig. 7 – HRTEM images of CNT/PAN (0.5 wt.% CNT) derived composite CNFs. (A) and (B) are typical distributions of graphitic planes in composite CNF mats. (C) Presence of a CNT in CNT–PAN composite CNF. (D) Higher graphitization near the walls of CNT in CNT/PAN derived CNF.

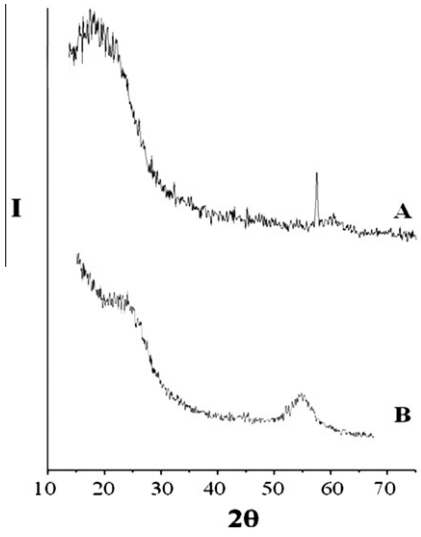

Fig. 8 – XRD spectra intensity for CNF derived from: (A) CNT/PAN composite, (B) pure PAN fibers.

nanoscale devices. Increased conductivity values, Raman spectra and XRD patterns in our study suggest that the modified electrical properties of pyrolyzed CNT/PAN nanofibers may be attributed to increased graphitization of carbon. Increased graphitization in CNF in this study is a combined effect of the fabrication technique, and the use of CNTs as an additive in the polymer precursor. The extent of carbonization and ordering of carbon atoms as stacked graphene sheets in a pyrolyzed electrospun polymer product may arise from the intrinsic and modified properties of the starting material, optimum pyrolysis conditions (e.g. final temperature, temperature ramp etc.), thickness of the fiber, mechanical pulling or stretching of the fiber, electrical field, flow conditions, and the evaporation rate of the solvent from nanofibers during electrospinning. We have, in the past, successfully achieved nanofibers in the 100 nm range with high aspect ratios by using controlled electrospinning of carbonizable polymers [43]. As a contribution to our ongoing efforts for obtaining ultrathin all graphite nanofibers we have attempted the fabrication of CNF by using a composite material with the templating effect resulting from CNTs.

The exact mechanism of nucleation and growth of graphitic crystals in carbonized CNT/PAN composites is still unclear, though it appears possible that CNTs can provide a template for graphitization and also increase the mechanical stresses generated by anisotropic thermal expansion during pyrolysis and accelerate the ordering of atoms. The resulting nanofiber material is more graphitic than the carbon obtained from the precursor polymer itself. It does not need any further purification and may be utilized directly for several electronics applications. The increased graphitization is evident in the HR-TEM pictures, Raman and XRD analyses and in the resulting higher conductivity of the fibers. In the HR-TEM pictures one does not observe network formation of CNTs, nor is there any sudden jump in the conductivity. Thus, the percolation point for the CNTs in the fibers is not reached, and it would seem that the increased conductivity is largely a result of enhanced graphitization.

As discussed earlier, the metal particles used for the growth of CNTs present in trace quantities were further dissolved by nitric acid treatment. To confirm that there are no traces of metal particles in CNT/PAN nanofibers, we also carried out thermo gravimetric analysis (TGA), which showed that there is no metal residue in the composite. Thus, the metallic impurities cannot contribute to greatly increased conductivity of the nanofibers.

Fabrication of carbon nanowires by using simple techniques such as electrospinning with highly graphitizable materials may well lead to inexpensive, versatile and scalable manufacturing techniques for next generation solid state electronics and sensor devices. Further work on uncovering the precise mechanisms of CNT induced templating is still required that will further help maximize the yield and homogeneity of graphite crystals.

5. Conclusions

We have used directed electrospinning of CNT/PAN solutions on photolithographically constructed SU 8 MEMS platforms to fabricate single suspended composite nanofibers that are subsequently pyrolyzed together with their polymeric platforms to form composite CNFs integrated on the carbon MEMS structures. These carbon nanowires anchored on micro-posts have the potential to be used as solid state sensors because their electrical properties can be directly addressed owing to their integration with the underlying micro-electrodes. The CNT/PAN solution concentration, chemical treatment of CNTs for better dispersion and the electrospinning parameters were optimized to form a sparse and directed network of suspended composite nanofibers anchored on the micro-posts. Formation of mats and entangled wires could be prevented.

The electrical conductivity of the composite carbon nanowires could be tuned by two orders of magnitude from 1.2×10^4 S/m to 3.10×10^6 S/m by an addition of 0.5 wt.% CNTs. This ability to control the electrical properties of the composite carbon nanowires over a wide range, together with their easy integration onto an underlying MEMS structure, should position them as a versatile advanced material for numerous electronic, sensor and inter-connect applications. The greatly increased conductivity also appears to correlate with the increased crystallinity of the CNT containing CNF that may have resulted from the nucleation and templating engendered by CNTs. More detailed investigations concerning the mechanism of CNT catalyzed graphitization in PAN and other carbonizable polymers is an interesting area for future investigations.

Acknowledgements

This work was supported by the Indo–US Center for Fabrionics at IIT Kanpur, India (Marc Madou and Ashutosh Sharma). The support of Ministry of Education, Science and Technology, South Korea under the World Class University (WCU) is acknowledged by Ashutosh Sharma under program R32-2008-000-20082-0 and by Yoon-Kyoung Cho and Marc Madou under R32-2008-000-20054-0.

REFERENCES

[1] IUPAC compendium of chemical terminology P. Recommended terminology for the description of carbon as a solid (IUPAC Recommendations 1995). Pure Appl Chem 1995;67:473–506.
[2] Spain IL. Electronics properties of graphite. In: Walker PLJ, Thrower PA, editors. Chemistry and Physics of Carbon, vol. 8. New York: Dekker; 1973. p. 87–94.
[3] Minot C. Graphite as an aromatic system. J Phys Chem 1987;91(25):6380–5.
[4] Novoselov KS, Geim AK, Morozov SV, Jiang D, Zhang Y, Dubonos SV, et al. Electric field effect in atomically thin carbon films. Science 2004;306(5696):666–9.
[5] Thess A, Lee R, Nikolaev P. Crystalline ropes of metallic carbon nanotubes. Science 1996;273(5274):483–7.
[6] Ra EJ, An KH, Kim KK, Jeong SY, Lee YH. Anisotropic electrical conductivity of MWCNT–PAN nanofiber paper. Chem Phys Lett 2005;413(1–3):188–93.
[7] Liu H, Kameoka J, Czaplewski DA, Craighead HG. Polymeric nanowire chemical sensor. Nano Lett 2004;4(4):671–5.
[8] Harfenist AS, Cambron SD, Nelson EW, Scott MB, Isham AW, Crain MM, et al. Direct drawing of suspended filamentary micro- and nanostructures from liquid polymers. Nano Lett 2004;4(10):1931–7.
[9] Coleman JN, Khan U, Blau WJ, Gunko YK. Small but strong: a review of the mechanical properties of carbon nanotube–polymer composites. Carbon 2006;44(9):1624–52.
[10] Donnet JB, Wang TK, Rebouillat S, Peng JC. Carbon Fibers. New York: Marcel Dekker Inc; 1998. p. 231–309.
[11] Chen IH, Wang CC, Chen CY. Fabrication and structural characterization of polyacrylonitrile and carbon nanofibers containing plasma-modified carbon nanotubes by electrospinning. J Phys Chem C 2010;114(32):13532–9.
[12] Wang C, Taherabadi L, Jia G, Madou M, Yeh Y, Dunnb B. C-MEMS for The manufacture of 3D microbatteries. Electrochem Solid State Lett 2004;7(11):A435–8.
[13] Kinoshita K. Carbons. In: Besenhard JO, editor. Handbook of Battery Materials. Weinheim: Wiley–VCH; 1999. p. 231–43.
[14] Hess M, Lebraud E, Levasseur A. Graphite multilayer thin films: a new anode material for Li-ion microbatteries synthesis and characterization. J Power Sources 1997;68(2):204–7.
[15] Wang JN, Zhao YZ, Niu JJ. Preparation of graphitic carbon with high surface area and its application as an electrode material for fuel cells. J Mater Chem 2007;17:2251–6.
[16] Sevilla M, Sanchis C, Valdes-Solis T, Morallon E, Fuertes AB. Direct synthesis of graphitic carbon nanostructures from saccharides and their use as electrocatalytic supports. Carbon 2008;46(6):931–9.
[17] Moafi A, Shafier M, Sadek AZ, Lau DWM, Partridge JG, Kalantar-Zadeh K, et al. IEEE Sensors Conference. 2010; p. 378–381.
[18] Li L, Lia J, Lukehart CM. Graphitic carbon nanofiber-poly(acrylate) polymer brushes as gas sensors. Sens Actuators B 2008;130(2):783–8.
[19] Oya A, Otani S. Catalytic graphitization of carbons by various metals. Carbon 1979;17(2):131–7.
[20] Oya A, Marsh H. Phenomena of catalytic graphitization. J Mat Sci 1982;17(2):309–22.
[21] Kruk M, Kohlhaas KM, Dufour B, Celer EB, Jaroniec M, Matyjaszewski K, et al. Partially graphitic, high-surface-area mesoporous carbons from polyacrylonitrile templated by ordered and disordered mesoporous silicas. Micropor Mesopor Mater 2007;102(1–3):178–87.
[22] Yang B, Marcus MS, Keppel DG, Zhang PP, Li ZW, Larson BJ, et al. Template-directed carbon nanotube network using self-organized Si nanocrystals. Appl Phys Lett 2005;86:263103–7.
[23] Wang H, Yao J. Use of poly(furfuryl alcohol) in the fabrication of nanostructured carbons and composites. Ind Eng Chem Res 2006;45(19):6393–404.
[24] Han S, Yun Y, Park KW, Sung YE, Hyeon TG. Simple solid-phase synthesis of hollow graphitic nanoparticles and their application to direct methanol fuel cell electrodes. Adv Mater 2003;15(22):1922–5.
[25] Zussman E, Chen X, Ding W, Calabri L, Dikin DA, Quintana JP, et al. Mechanical and structural characterization of electrospun PAN-derived carbon nanofibers. Carbon 2005;43(10):2175–85.
[26] Sulong AB, Muhamad N, Sahari J, Ramli R, Deros BM, Park J. Electrical conductivity behavior of chemical functionalized MWCNTs epoxy composites. Eur J Sci Res 2009;29(1): 13–21.
[27] Khare R, Bose S. Carbon nanotube based composites-a review. J Miner Mater Charact Eng 2005;4(1):31–46.
[28] Guo H, Minus ML, Jagannathan S, Kumar S. Polyacrylonitrile/carbon nanotube composite films. ACS Appl Mat Interfaces 2010;2(5):1331–42.
[29] Chae HG, Choi YH, Minus ML, Kumar S. Carbon nanotube reinforced small diameter polyacrylonitrile based carbon fiber. Compos Sci Technol 2009;69(3–4):406–13.
[30] Breuer O, Sundararaj U. Big returns from small fibers: a review of polymer/carbon nanotube composite. Polym Compos 2004;25(6):630–45.
[31] Bibekananda S, Babu VJ, Subramanian V, Natarajan TS. Preparation and characterization of electrospun fibers of poly(methyl methacrylate) – single walled carbon nanotube composites. J Eng Fibers Fabr 2008;3(4):40–5.
[32] Bal S, Samal SS. Carbon nanotube reinforced polymer composites-A state of the art. Bull Mater Sci 2007;30(4):379–86.
[33] Ryan KP, Cadek M, Nicolosi V, Blond D, Ruether M, GA G, et al. Carbon nanotubes for reinforcement of plastics? A case study with poly(vinyl alcohol). Compos Sci Technol 2007;67(7–8):1640–9.
[34] Minus ML, Chae HG, Kumar S. Interfacial crystallization in gel-spun poly(vinyl alcohol)/single-wall carbon nanotube composite fibers. Macromol Chem Phys 2009;210(21):1799–808.
[35] Chae HG, Sreekumar TV, Uchida T, Kumar S. A comparison of reinforcement efficiency of various types of carbon nanotubes in polyacrylonitrile fiber. Polymer 2005;46(24):10925–35.
[36] Chae HG, Minus ML, Rasheed A, Kumar S. Stabilization and carbonization of gel spun polyacrylonitrile/single wall carbon nanotube composite fibers. Polymer 2007;48(13):3781–9.
[37] Chae HG, Minus ML, Kumar S. Oriented and exfoliated single wall carbon nanotubes in polyacrylonitrile. Polym Compos 2006;47(10):3494–505.
[38] Prshantha K, Soulestin J, Lacrampe MF, Krawczak P. Present status and key challenges of carbon nanotubes reinforced polyolefins: a review on composites manufacturing and performance issues. Polym Compos 2009;17(4):205–45.
[39] Peijs T, Vught RJMV, Govaert LE. Mechanical properties of poly(vinyl alcohol) fibres and composites. Compos Sci Technol 1995;26(2):83–90.
[40] Dalton AB, Collins S, Munoz E, Razal JM, Ebron VH, Ferraris JP, et al. Super-tough carbon-nanotube fibres. Nature 2003;423. 703.
[41] Ryu Z, Zheng J, Wang M, Zhang B. Nitrogen adsorption studies of PAN-based activated carbon fibers prepared by different activation methods. J Colloid Interface Sci 2000;230(2):312–9.

[42] Malladi K, Wang C, Madou M. Fabrication of suspended carbon microstructures by e-beam writer and pyrolysis. Carbon 2006;44(13):2602–7.
[43] Sharma CS, Katepalli H, Sharma A, Madou M. Fabrication and electrical conductivity of suspended carbon nanofiber arrays. Carbon 2011;49(5):1727–32.
[44] Garcia RE, Chiang YM, Carter WC, Limthongkul P, Bishop CM. Microstructural modeling and design of rechargeable lithium-ion batteries. J Electrochem Soc 2005;152(1): A255–63.
[45] Mukhopadhyay K, Koshio A, Sugai T, Tanaka N, Shinohara H, Konya Z. Bulk production of quasi-aligned carbon nanotube bundles by the catalytic chemical vapor deposition (CCVD) method. Chem Phys Lett 1999;303:117–24.
[46] Knight D, White WB. Characterization of diamond films by Raman spectroscopy. J Mass Spectrom 1989;4(2):385–93.